PROCEEDINGS OF SCIENCE

New results on Parton Densities of Nucleons and Nuclei

Stefan Schmitt*
DESY, Hamburg
E-mail: Stefan.Schmitt@desy.de

Following the concept of QCD collinear factorisation, collisions involving nucleons or nuclei are commonly described with the help of collinear parton density functions (PDFs). The PDFs are often determined in fits to a variety of datasets. This article is giving an overview of recent developments in the field of PDF determination, with emphasis on results from collider experiments.

XXVI International Workshop on Deep-Inelastic Scattering and Related Subjects (DIS2018)
16-20 April 2018
Kobe, Japan

*Speaker.

PoS(DIS2018)233

1. Introduction

1.1 Collinear QCD factorisation

High-energy collisions involving at least one hadron are often described with the help of collinear QCD factorisation [1]. Examples are sketched in Figure 1. Perhaps the simplest case is inclusive deep-inelastic scattering (DIS), where the cross section is schematically written as

$$\sigma_{ep\to eX} \sim \sum_i f_i \otimes |M_i|^2 + \text{higher twist} \qquad (1.1)$$

The initial state hadron is described by parton density functions (PDFs) f_i. These are for a given hadron process-independent functions $f_i = f_i(x,\mu)$ of the hard scale μ, a convolution variable x and a flavour index i. For predicting DIS cross sections, the PDFs are convoluted with coefficient functions $|M_i|^2$. These are specific to the process studied and include the measurement function, but are independent of the initial state hadron. They can be calculated in QCD perturbation theory. Another example process is the case of semi-inclusive DIS, where the production of a hadron h in the final state is studied. The factorisation then includes a second convolution process, involving fragmentation functions (FFs). These describe the transition from partons to the selected hadron. A third example are collisions with two hadrons in the initial state. In this case, coefficient functions are convoluted with two PDFs to predict cross sections. Contributions to the cross sections not predicted by convolution of PDFs with coefficient functions are "higher twist". QCD factorisation is said to be "valid" if the higher-twist terms are suppressed by powers $1/\mu^N$ of the hard scale, with $N \geq 1$. The validity of QCD factorisation is proven only for a selection of hard processes, such as inclusive, semi-inclusive and diffractive deep-inelastic scattering or Drell-Yan, W, jet and heavy flavour production in collisions of two hadrons.

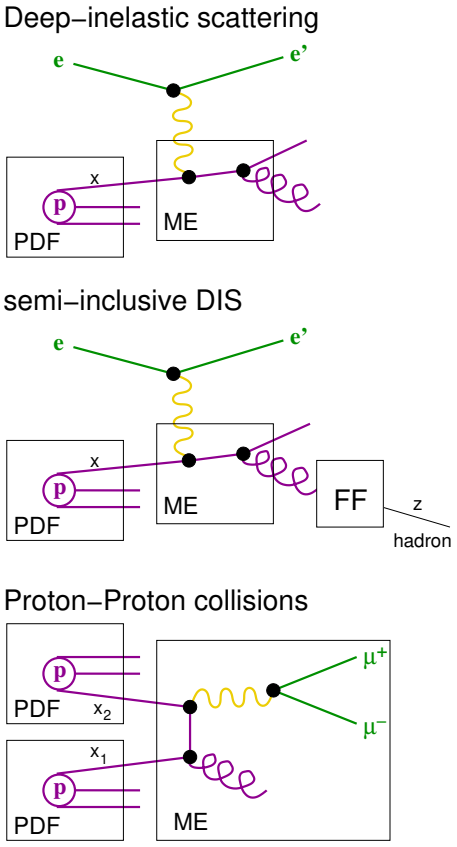

Figure 1: Examples of processes described with the help of collinear QCD factorisation: inclusive deep-inelastic scattering (DIS), semi-inclusive DIS (sDIS) and Drell-Yan production.

1.2 PDF evolution

In a simplified picture the PDFs $f_i(x,\mu^2)$ describe the probability to find a parton of flavor i and longitudinal momentum fraction x in the incoming hadron, given the hard scale μ. The DGLAP equations [2, 3, 4] describe how a given set of parton density functions $f_i(x,\mu_0)$, known at a fixed scale μ_0, is evolved to a another scale $\mu \neq \mu_0$, given the running QCD coupling $\alpha_s(\mu)$. In other words, instead of having to know the PDFs as a function of two variables $f_i(x,\mu)$, it is

sufficient to know the PDFs as a function of a single variable x for a fixed (and arbitrary) scale μ_0. The DGLAP evolution is an essential ingredient to extract PDFs from measured cross sections in QCD fits. The PDF evolution equations and the coefficient functions of many processes are known beyond leading order, such that modern QCD fits are routinely done in next-to-leading order (NLO) or next-to-next-to-leading order (NNLO) QCD. Figure 2 shows recent PDF fits by the NNPDF collaboration [5] at scales $\mu = 3.16\,\text{GeV}$ and $\mu = 100\,\text{GeV}$.

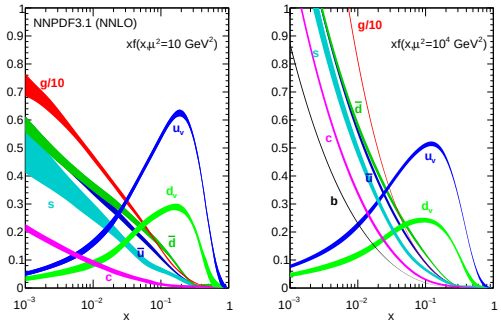

Figure 2: NNPDF3.1 Parton density functions shown at two different scales. Figure source: arXiv.org [5].

1.3 PDF fits

Parton density functions are extracted from data in PDF fits. For such fits, the PDFs are parameterised at a starting scale μ_0. The functions $f_i(x,\mu_0)$ at the scale μ_0 are typically described by a finite number of parameters. When fixing these PDF parameters and the strong coupling $\alpha_s(m_Z)$, as well as other parameters such as the heavy quark masses, cross sections can be predicted for any process where the coefficient functions are available. By minimising the deviations of the predictions from measurements, estimates of the PDF parameters can be determined in a fit. The data uncertainties correspondingly translate to uncertainties on the resulting PDF parameters.

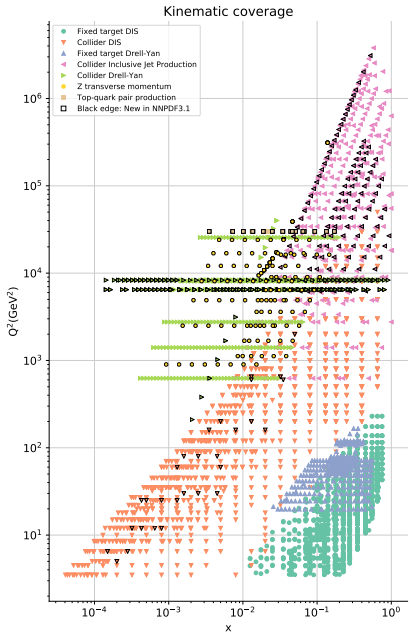

Figure 3: Datasets used for the NNPDF3.1 parton density functions in the kinematic plane. Figure source: arXiv.org [5].

Such PDF fits are carried out by different groups, using different sets of input data and different ways to parameterise the PDFs at the starting scale. The backbone of most PDF fits are the inclusive HERA data [6], cross section measurements of neutral-current and charged-current deep-inelastic scattering at $\sqrt{s} = 320\,\text{GeV}$ covering different lepton charges and a wide range in x-Bjorken and negative four-momentum transfer squared Q^2. The HERA data also include smaller samples of neutral-current data at reduced centre-of-mass energies, thus enhancing the sensitivity to the gluon at low x through the structure function F_L. Figure 3 shows an overview of the datasets included in the NNPDF3.1 fit [5] in the kinematic plane.

2. New results in deep-inelastic scattering

2.1 Low-x resummation

The HERA data [6] have been poorly described by PDF fits in the region of small x and low Q^2. The convergence of fixed-order calculations possibly can be improved in this kinematic regime by low-x resummation. Calculations of splitting functions and coefficient functions with re-summed low-x terms have recently been made available as computer code [7] for use in PDF fits. The PDFs are characterised by a stronger increase of the gluon and sea quark contributions with low x [8]. The description of the low x HERA data is improved significantly, as well as the description of measurements of charm production at HERA [8, 9]. Comparisons of NNLO PDF fits with and without low-x resummation to HERA inclusive data [9] are shown in figure 4.

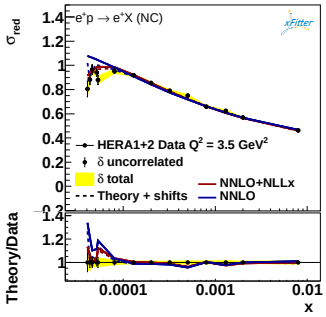

Figure 4: HERA data at $Q^2 = 3.5\,\mathrm{GeV}^2$ compared to NNLO QCD fits with and without low-x resummation. Figure source: arXiv.org [9].

2.2 Charm and beauty at HERA

A new combination of charm and beauty measurements at HERA [10] was published recently, improving in precision over the previous combination of charm data only [11]. It is theoretically challenging to describe heavy flavour production at HERA, as there are several hard scales involved, such as the momentum transfer Q, the heavy quark masses m_c and m_b and transverse momenta of the final state. For combining the various HERA datasets collected by the H1 and ZEUS experiments, fiducial measurements are extrapolated to the full phase-space. All measurements are then averaged and good consistency of the datasets is observed. The charm data have uncertainties reduced by typically 20% as compared to the previous HERA combination. The beauty data are combined for the first time. The combined data are compared in figure 5 to NLO calculations in the fixed-flavour-number scheme, which are most appropriate for describing DIS heavy-flavour production at scales in the vicinity of the heavy quark masses. Overall the measurements are well described by the calculations, but there are deviations in the x-Bjorken distributions near $Q^2 = 12\,\mathrm{GeV}^2$. The same is true for variable-flavour-number scheme calculations. However, the overall deviation is of

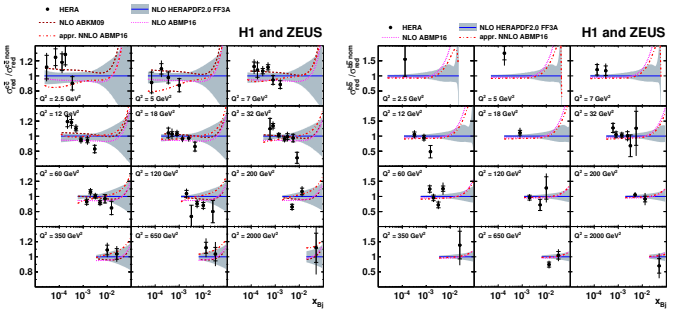

Figure 5: HERA combined data on charm and beauty production, relative to the HERAPDF2.0FF3A NLO QCD prediction. Figure source: arXiv.org [10].

order three standard deviations only. A PDF fit of the combined charm and beauty data together with the combined inclusive HERA data is performed in which the charm and beauty quark masses are free parameters in addition to the PDF parameters. The resulting heavy quark masses are found to be

$$m_c(m_c) = 1.290^{+0.077}_{-0.053}\,\text{GeV} \quad \text{and} \quad m_b(m_b) = 4.049^{+0.138}_{-0.118}\,\text{GeV}, \tag{2.1}$$

in good agreement with the world averages. Further studies are made [10] to compare the data to recent predictions based on low-x resummation. As compared to the calculations presented above, the predicted shapes in x are in better agreement with data, however the Q^2 dependencies are less well modelled.

2.3 Jet production at HERA

The H1 collaboration recently published determinations of the strong coupling $\alpha_s(M_z)$ from jet data in DIS [12] using NNLO QCD predictions [13, 14]. One out of the methods advertised in that paper is the simultaneous determination of the strong coupling constant and PDF parameters using H1 inclusive and H1 jet data together. The strong coupling is determined in that fit as

$$\alpha_s(m_Z) = 0.1142(28) \tag{2.2}$$

The use of the H1 jet data in the fit enables a simultaneous determination of $\alpha_s(m_Z)$ and parameters describing the gluon density from H1 data alone. Figure 6 shows the gluon density and the correlation between the gluon density and α_s. While α_s is a bit lower than the world average, the gluon and singlet contributions are correspondingly somewhat larger than in other PDF fits. The correlation with α_s is reduced significantly, as compared to a fit without jet data.

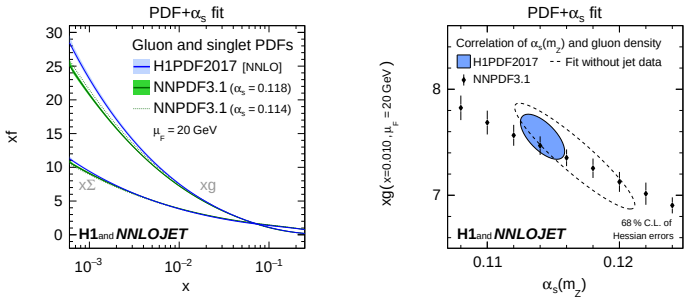

Figure 6: Gluon and singlet density and correlation of the gluon density and the strong coupling determined in a fit to H1 inclusive DIS and jet data. Figure source: arXiv.org [12].

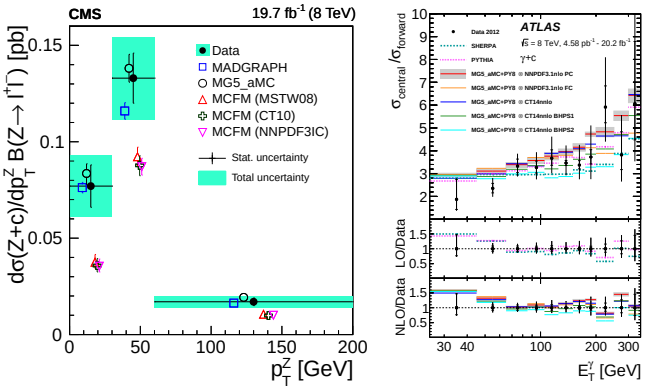

Figure 7: Measurements of $c+Z$ and $c+\gamma$ production at the LHC, compared to predictions. Figure source: arXiv.org [16, 17].

3. Probing intrinsic charm

Recent PDF fits [5, 15] explore constraints on a possible intrinsic charm component in the proton for scales $\mu > m_c$, which would contribute in addition to the perturbative charm contribution from gluon splitting. Predictions by CTEQ-TEA on the production of charm in association with a Z-boson at the LHC indicate that such measurements may be able to constrain the magnitude of intrinsic charm contributions in the future. Measurements by CMS on Z plus charm [16] and by ATLAS on photon plus charm [17] are shown in figure 7. While the Z channel is still statistically limited, the photon channel is starting to discriminate between models. However, as shown in the CMS analysis, details in the QCD modelling do complicate a precision analysis.

4. High-x gluon, valence quarks

4.1 Jet production in pp collisions

Jet production in pp collisions at the LHC can be used to probe QCD at high scales and high x, given the large data samples recorded. The ATLAS collaboration published double-differential inclusive jet cross section measurements at centre-of-mass energies $\sqrt{s} = 8$ and $\sqrt{s} = 13\,\text{TeV}$, as well as dijet cross section measurements at $\sqrt{s} = 13\,\text{TeV}$ [18, 19]. The CMS collaboration presented triple-differential measurements of dijet cross sections at $\sqrt{s} = 8\,\text{TeV}$ [20]. As compared to double-differential measurements, the triple differential measurements have further enhanced sensitivity to PDFs. Figure 8 shows the measurements and their impact on constraining the high-x gluon and valence quark distributions.

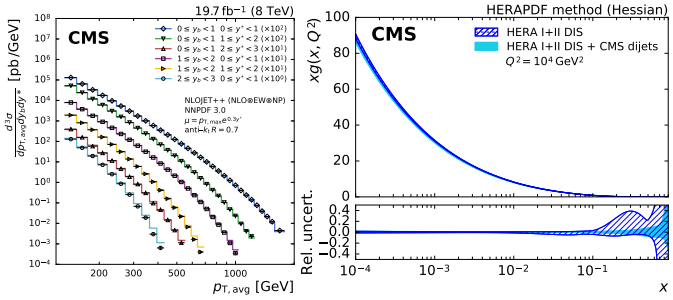

Figure 8: Triple-differential measurement of dijet production by CMS. Figure source: arXiv.org [20].

.

LHC jet data measured at $\sqrt{s} = 7\,\text{TeV}$ have been included in a global PDF fit at NNLO [21] by the MMHT group [22]. The relative uncertainty on the gluon is reduced by up to 20% when including jet data from both Tevatron and the LHC. For some of the datasets, difficulties to accommodate the default correlation model of the systematic uncertainties are reported.

4.2 Top quark pair production

Due to the large top quark mass, top pair production naturally probes the gluon PDF at large scales and large x. The integrated cross section alone already adds significant information at high x, due to missing constraints in this regions from HERA data alone. Measurements by CMS as a function of the centre-of-mass energy [23] and measurements in the forward direction by LHCb [24] could be included in future PDF fits. Normalised single-differential cross sections as reported by ATLAS [25] and double-differential cross sections as reported by CMS [26] have the

potential to further constrain the gluon at high x. This is illustrated in Figure 9, where the impact on the gluon density by including normalised double differential cross sections is illustrated.

5. Flavour separation and strangeness

5.1 Constraints from LHC data

The HERA DIS data alone have limited power to constrain the strange quark density. In the HERAPDF fits, the strange distribution was taken to be equal to a fixed "suppression factor" relative to the (anti-)down sea quark density. Fixed target experiments such as HERMES were able to extract an x-dependent strangeness suppression from sDIS data [27], however the analysis was performed in leading-order only. As precision data on Drell-Yan and W production at the LHC is becoming available, several groups are doing PDF fits with emphasis of analysing the strange-quark content of the proton. Already in 2012, the ATLAS collaboration reported an analysis of their data, which gave evidence for a non-suppressed strange sea [28]. In contrast, the CMS collaboration analysed data on W^+-W^- asymmetries in 2013 [29] and found evidence for a suppressed strange sea. Both collaborations also measured the production of W plus charm [30, 31], which is more directly sensitive to strange quarks in the proton. The ATLAS result again preferred an unsuppressed strangeness, whereas the CMS result was better compatible with strangeness suppression.

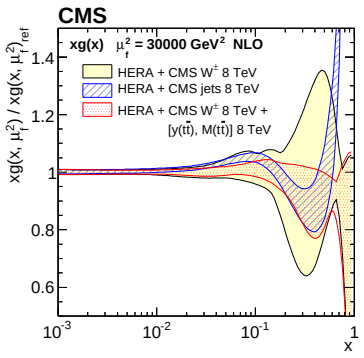

Figure 9: Gluon PDF constrained by CMS double-differential $t\bar{t}$ measurements. Figure source: arXiv.org [26].

The ATLAS collaboration recently published precision measurements of Drell-Yan and W production [32, 33]. The measured cross sections have bin-to-bin uncorrelated uncertainties smaller than 1% and normalisation uncertainties of 1.8%. The ATLAS PDF fit again prefers an unsuppressed strange sea. However, as shown in figure 10, the PDF parameterisation has sizeable shape uncertainties not constrained by the Drell-Yan and W data. The CMS collaboration showed a new measurement on W plus charm production [34]. This measurement prefers a shape which is different from the ATLAS default parameterisation. Other groups have studied the LHC data sensitive to strangeness in independent analyses. ATLAS and CMS data on Drell-Yan and W production seem to be compatible with each other when analysed with identical PDF parameterisations [35]. The ABM group

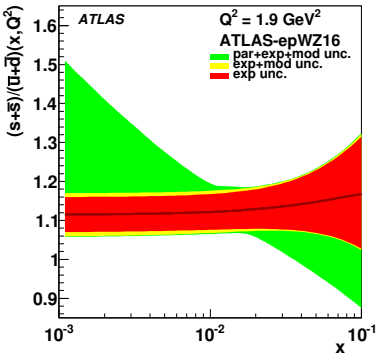

Figure 10: Strangeness PDF extracted by ATLAS using their Drell-Yan and W production data. Figure source: arXiv.org [32].

analysed the constraints imposed by the ATLAS parameterisations in greater detail [36]. They argue that that parameterisation is not flexible enough and imposes unphysical constraints which are, for example, incompatible with fixed-target E866 data on $\bar{d}/\bar{u}$ [37].

5.2 Prospects on flavour separation from non-collider data

The SeaQuest collaboration is aiming to improve the over E866 measurements on $\bar{d}/\bar{u}$ [37], using data recorded at smaller centre-of mass energies. Preliminary results are available [38].

JLAB has a large program set up to to measure polarised and unpolarised deep-inelastic scattering in various targets. In hall C, precision measurements of the structure function F_2 in ep and ed are ongoing. Many new experiments are planned to run at an electron beam energy of 12 GeV. The MARATHON experiment is aiming to measure cross sections on ^{3}H and ^{3}He targets, where nuclear corrections cancel in the ratios. The BONus12 experiment is going to tag recoil protons and hence provides measurement on an effective free neutron target. The SoLID PVDIS experiment is aiming for measurements of the u/d ratio in parity-violating ep scattering.

Another interesting project is the extraction of parton densities from lattice-QCD calculations. Two groups [39, 40] recently reported results on the differences $u-d$ and $\bar{u}-\bar{d}$ from calculations which can be compared directly to PDF fits.

6. Nuclear PDFs

PDF parameterisations for nuclei other than the proton are often references as "nuclear" PDFs (nPDFs). Recent nPDF fits [42, 43] are based on free proton PDFs. By invoking isospin-asymmetry, PDFs for the free neutron can be predicted by swapping the role of up and down quarks. These free proton and free neutron PDFs are then multiplied by the number of protons Z and the number of neutrons $A-Z$, respectively, and the results are added up. Effects arising from the fact that the protons and neutrons are bound in the nucleus are taken into account using "nuclear modification factors". These depend on the atomic number A, the flavour and the momentum fraction x. Here, the momentum fraction x for nPDFs is given relative to a single nucleon, such that x/A would correspond to the momentum fraction relative to the whole nucleus. An example nuclear modification factor is shown in figure 11. For small x, the factor is below unity, corresponding to the "shadowing" region. Near $x = 0.1$ the modification is above unity in the "anti-shadowing" region. Near $x = 0.5$ the modification is again below unity, the so-called "EMC effect". Towards $x = 1$ the factor rises to very large numbers.

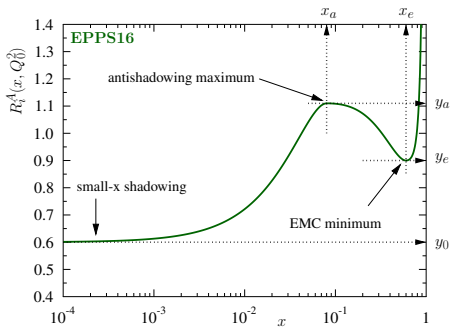

Figure 11: Nuclear modification factor as used in the EPPS16 nPDF fit. Figure source: arXiv.org [43].

6.1 LHC pA and AA Drell-Yan and W data in global fits

Precision measurements of structure functions and Drell-Yan cross sections with various nuclear targets are the basis of nPDF extractions [42]. Measurements of Drell-Yan and W production at the LHC have been included in nPDF fits, thus extending the kinematic region constrained by data to lower x. The EPPS16 fit [43] and a recent study by nCTEQ [44] quantify how LHC data from *p-Pb* collisions at $\sqrt{s} = 5.02\,\text{GeV}$ and *Pb-Pb* collisions at $\sqrt{s} = 2.76\,\text{GeV}$ compare to nPDF fits not using LHC data.

New data on forward W and Z production in *p-Pb* collisions at $\sqrt{s} = 5.02\,\text{TeV}$ and on forward Z production have been released by the ALICE collaboration [45]. They are shown together with data measured by the other LHC experiments in figure 12. Predictions based on pre-LHC nPDFs are in fair agreement with the measurements. New ALICE data on forward Z production in *Pb-Pb* collisions at $\sqrt{s} = 5.02\,\text{TeV}$ [46] also have been tested against predictions. While the EPPS16 nPDFs are able to describe the data, predictions based on free nucleons fail to describe these.

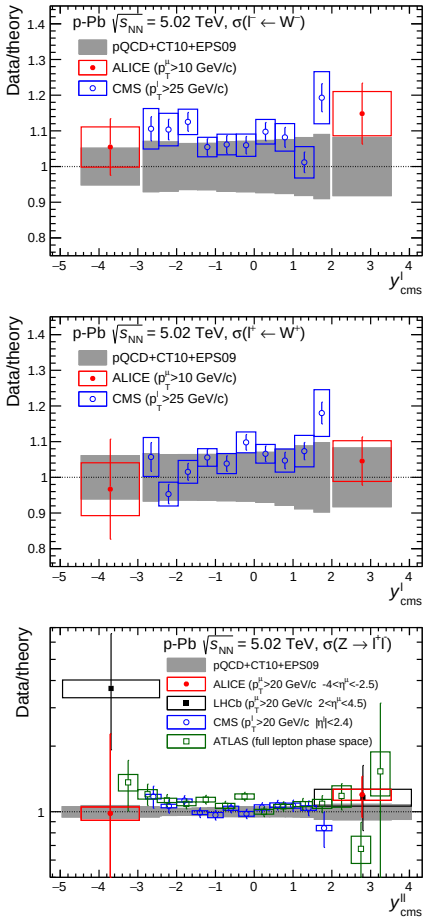

Figure 12: Data on forward and central W and Z production at the LHC in *p-Pb* collisions at $\sqrt{s} = 5.02\,\text{TeV}$. Figure source: arXiv.org [45].

6.2 Including pA and AA heavy-flavour data in nuclear PDFs

Measuring charm and beauty has a long tradition in heavy-ion collisions. A wealth of such measurements is available in *p-Pb* and *Pb-Pb* collisions at the LHC for various centre-of-mass energies. A recent study [47] is exploring in a systematic way the compatibility of these measurements with recent nPDF fits. The possible impact of these data on future nPDF fits is quantified and is expected to be significant.

7. Summary

More than forty years after writing down the DGLAP equations, investigations of parton densities are still under active developments. The field is driven both by new measurements and by advancements in theory. The review presented here is trying to highlight a few recent developments, with emphasis on experimental results and predictions which can be compared directly to new data.

Low-x resummation is now available for PDF fits in a publicly available computer code. This has triggered several investigations on HERA precision

data both in inclusive DIS and in charm and beauty production. Future investigations may profit from the updated combination of charm and beauty data which was presented by the H1 and ZEUS collaborations.

LHC measurements of jet production at high transverse momenta and of top quark production are interesting for constraining PDFs, in particular the gluon density, at high x. Drell-Yan and W production is measured multi-differentially and is important for separating the quark flavours in the sea. Together with measurements of W plus charm, more flexible PDF parameterisations can be probed, thus refining the knowledge about the x dependence of the strange sea. New data on c with a photon or Z boson are starting to become sensitive to the question whether an intrinsic charm component is required to describe charm in the proton. It is worth noting that the sensitivity of new LHC data to PDFs in many cases is quantified in dedicated PDF fit studies performed by the authors themselves, which in turn is useful for progress on global PDF extractions based on many datasets.

LHC data also has started to become important for fits of PDFs of nuclear targets. Data on W and Z production are already included in such recent global fits. The compatibility of global nuclear PDF fits with data on heavy-flavour production also has been studied. It seems promising to include these data in future nuclear PDF fits.

References

[1] J. C. Collins, D. E. Soper and G. F. Sterman, Adv. Ser. Direct. High Energy Phys. **5** (1989) 1 [hep-ph/0409313].

[2] V. N. Gribov and L. N. Lipatov, *Sov. J. Nucl. Phys.* 15 (1972) 438. [Yad. Fiz. 15 (1972) 781].

[3] G. Altarelli and G. Parisi, Nucl. Phys. B **126** (1977) 298.

[4] Y. L. Dokshitzer, *Sov. Phys. JETP* 46 (1977) 641. [Zh. Eksp. Teor. Fiz. 73 (1977) 1216].

[5] R. D. Ball *et al.* [NNPDF Collaboration], Eur. Phys. J. C **77** (2017) 663 [arXiv:1706.00428].

[6] H. Abramowicz *et al.* [H1 and ZEUS Collaborations], Eur. Phys. J. C **75** (2015) 580 [arXiv:1506.06042].

[7] M. Bonvini, S. Marzani and C. Muselli, JHEP **1712** (2017) 117 [arXiv:1708.07510].

[8] R. D. Ball, V. Bertone, M. Bonvini, S. Marzani, J. Rojo and L. Rottoli, Eur. Phys. J. C **78** (2018) 321 [arXiv:1710.05935].

[9] H. Abdolmaleki *et al.* [xFitter Developers' Team], Eur. Phys. J. C **78** (2018) 621 [arXiv:1802.00064].

[10] H. Abramowicz *et al.* [H1 and ZEUS Collaborations], Eur. Phys. J. C **78** (2018) 473 [arXiv:1804.01019].

[11] H. Abramowicz *et al.* [H1 and ZEUS Collaborations], Eur. Phys. J. C **73** (2013) 2311 [arXiv:1211.1182].

[12] V. Andreev *et al.* [H1 Collaboration], Eur. Phys. J. C **77** (2017) 791 [arXiv:1709.07251].

[13] J. Currie, T. Gehrmann and J. Niehues, Phys. Rev. Lett. **117** (2016) 042001 [arXiv:1606.03991].

[14] J. Currie, T. Gehrmann, A. Huss and J. Niehues, JHEP **1707** (2017) 018 [arXiv:1703.05977].

[15] T. J. Hou *et al.*, JHEP **1802** (2018) 059 [arXiv:1707.00657].

[16] A. M. Sirunyan *et al.* [CMS Collaboration], Eur. Phys. J. C **78** (2018) 287 [arXiv:1711.02143].

[17] M. Aaboud *et al.* [ATLAS Collaboration], Phys. Lett. B **776** (2018) 295 [arXiv:1710.09560].

[18] M. Aaboud *et al.* [ATLAS Collaboration], JHEP **1709** (2017) 020 [arXiv:1706.03192].

[19] M. Aaboud *et al.* [ATLAS Collaboration], JHEP **1805** (2018) 195 [arXiv:1711.02692].

[20] A. M. Sirunyan *et al.* [CMS Collaboration], Eur. Phys. J. C **77** (2017) 746 [arXiv:1705.02628].

[21] J. Currie, E. W. N. Glover and J. Pires, Phys. Rev. Lett. **118** (2017) 072002 [arXiv:1611.01460].

[22] L. A. Harland-Lang, A. D. Martin and R. S. Thorne, Eur. Phys. J. C **78** (2018) 248 [arXiv:1711.05757].

[23] A. M. Sirunyan *et al.* [CMS Collaboration], JHEP **1803** (2018) 115 [arXiv:1711.03143].

[24] R. Aaij *et al.* [LHCb Collaboration], arXiv:1803.05188.

[25] M. Aaboud *et al.* [ATLAS Collaboration], Eur. Phys. J. C **77** (2017) 804 [arXiv:1709.09407].

[26] A. M. Sirunyan *et al.* [CMS Collaboration], Eur. Phys. J. C **77** (2017) 459 [arXiv:1703.01630].

[27] A. Airapetian *et al.* [HERMES Collaboration], Phys. Rev. D **89** (2014) 097101 [arXiv:1312.7028].

[28] G. Aad *et al.* [ATLAS Collaboration], Phys. Rev. Lett. **109** (2012) 012001 [arXiv:1203.4051].

[29] S. Chatrchyan *et al.* [CMS Collaboration], Phys. Rev. D **90** (2014) 032004 [arXiv:1312.6283].

[30] S. Chatrchyan *et al.* [CMS Collaboration], JHEP **1402** (2014) 013 [arXiv:1310.1138].

[31] G. Aad *et al.* [ATLAS Collaboration], JHEP **1405** (2014) 068 [arXiv:1402.6263].

[32] M. Aaboud *et al.* [ATLAS Collaboration], Eur. Phys. J. C **77** (2017) 367 [arXiv:1612.03016].

[33] M. Aaboud *et al.* [ATLAS Collaboration], JHEP **1712** (2017) 059 [arXiv:1710.05167].

[34] CMS Collaboration [CMS Collaboration], CMS-PAS-SMP-17-014.

[35] A. M. Cooper-Sarkar and K. Wichmann, Phys. Rev. D **98** (2018) 014027 [arXiv:1803.00968].

[36] S. Alekhin, J. Blümlein and S. Moch, Phys. Lett. B **777** (2018) 134 [arXiv:1708.01067].

[37] R. S. Towell *et al.* [NuSea Collaboration], Phys. Rev. D **64** (2001) 052002 [hep-ex/0103030].

[38] K. Nagai, JPS Conf. Proc. **13** (2017) 020051.

[39] C. Alexandrou, K. Cichy, M. Constantinou, K. Jansen, A. Scapellato and F. Steffens, arXiv:1803.02685.

[40] J. W. Chen, L. Jin, H. W. Lin, Y. S. Liu, Y. B. Yang, J. H. Zhang and Y. Zhao, arXiv:1803.04393.

[41] S. Dulat *et al.*, Phys. Rev. D **93** (2016) 033006 [arXiv:1506.07443].

[42] K. Kovarik *et al.*, Phys. Rev. D **93** (2016) 085037 [arXiv:1509.00792].

[43] K. J. Eskola, P. Paakkinen, H. Paukkunen and C. A. Salgado, Eur. Phys. J. C **77** (2017) 163 [arXiv:1612.05741].

[44] A. Kusina *et al.*, Eur. Phys. J. C **77** (2017) 488 [arXiv:1610.02925 [nucl-th]].

[45] J. Adam *et al.* [ALICE Collaboration], JHEP **1702** (2017) 077 [arXiv:1611.03002 [nucl-ex]].

[46] S. Acharya *et al.* [ALICE Collaboration], Phys. Lett. B **780** (2018) 372 [arXiv:1711.10753 [nucl-ex]].

[47] A. Kusina, J. P. Lansberg, I. Schienbein and H. S. Shao, Phys. Rev. Lett. **121** (2018) 052004 [arXiv:1712.07024].